

Control of Nanoparticle Location in Block Copolymers

Julia J. Chiu,[†] Bumjoon J. Kim,[†] Edward J. Kramer,^{*,†,‡} and David J. Pine^{*,†,‡}*Departments of Chemical Engineering and Materials, University of California, Santa Barbara, California 93106*

Received February 1, 2005; E-mail: edkramer@mrl.ucsb.edu; pine@mrl.ucsb.edu

Incorporating nanoparticles into a polymer matrix can have a significant impact on a wide range of material properties, including mechanical strength, conductivity, permeability, catalytic activity, and optical and magnetic properties. While these properties generally depend on how the particles are dispersed within the polymer matrix, the ability to control the arrangement of particles is limited. Recently, it has been suggested that block copolymers, with their rich diversity of structures at nanometer length scales, may provide an effective means for controlling particle location and patterns.^{1–3} To this end, a variety of methods have been developed to selectively incorporate nanoparticles into the desired block copolymer domains.^{4–10} However, success in controlling their precise location within the domains remains limited.

In this communication, we demonstrate a simple procedure to incorporate nanoparticles and control their location within different diblock copolymer domains by controlling the surface chemistry of the particles. To localize particles within the A- or B-domain of an A–B block copolymer, particles are coated with either A or B-type homopolymer, respectively. To localize particles at the interfaces between the blocks, particles are coated with a mixture of A- and B-type homopolymers. Using this approach, the particles can be localized entirely within one copolymer domain or the other, or they can be localized at the interfaces between the blocks.

For a copolymer, we use symmetric poly(styrene-*b*-2 vinyl pyridine) (PS-PVP) diblock copolymer with a total molecular weight of $M_n \sim 196\,500$ g/mol and a polydispersity of 1.11 (Polymer Source, Inc.). PS- and PVP-coated gold particles are synthesized by standard reduction of $\text{HAuCl}_4 \cdot 3\text{H}_2\text{O}$ in THF¹¹ or two phase toluene/water¹² utilizing thiol-terminated PS ($M_n \sim 1300$ g/mol, PDI = 1.10) and PVP ($M_n \sim 1500$ g/mol, PDI = 1.09) stabilizing ligands, respectively. For particles coated with both PS and PVP chains, a 1:1 molar mixture of PS:PVP thiol is added to the synthesis batch in THF. Particles are purified by membrane filtration (MWCO 30 000 Dalton, Millipore, Inc.) using dimethyl formamide as a solvent and are subsequently washed with methanol to remove any unbound thiol and residual reducing agent. The thiol-terminated PS and PVP ligands are synthesized by standard anionic polymerization followed by reaction of the polyanion with propylene sulfide.¹³ The molecular weights of the thiol ligands are determined by GPC and confirmed by NMR end group analysis. Grafting densities for various core–shell-type particles are estimated based on the weight fractions of gold and polymer ligands obtained from elemental analysis (Huffman Laboratories, Inc. Golden, CO).

To prepare the polymer–nanoparticle composites, we typically prepare a 2 wt % polymer solution in dichloromethane admixed with PS-coated gold particles having a volume fraction of 0.15 in the solid. A particle/polymer composite is prepared by solvent casting a mixture of nanoparticles and polymer in dichloromethane onto an epoxy substrate and then annealing under a saturated solvent atmosphere at 25 °C. The solvent annealing time is usually 1 day

followed by 1 day of slow drying in air. Subsequent removal of any residual solvent is carried out under vacuum for an additional minimum of 4 h. Particle size and gold particle location are determined by transmission electron microscopy (TEM) using a FEI T20 microscope operated at 200 kV. Samples are prepared for cross-sectional TEM by microtoming epoxy-supported bulk films and, in some cases, by subsequent selective staining of the PVP domains using iodine.

The average particle core (Au) diameters determined from TEM are found to be similar for all batches of gold including PS-, PVP-, and PS/PVP-coated particles synthesized in THF or toluene. In Figure 1, we show a TEM image of PS-coated particles and the corresponding histogram of their size distribution. The average core diameter is estimated to be 3.9 ± 1.0 nm, obtained by analyzing more than 200 particles using standard image analysis software. The polymer shell thickness, which is estimated from the distance between particles arranged in a monolayer film on the TEM grid, is approximately 1.9 nm. Thus, the diameter of the particles d (core + shell) is 7.7 ± 1.0 nm.

Figure 2a shows a TEM micrograph of PS-coated particles dispersed in a PS-PVP lamellar diblock copolymer phase. From the figure, it is clear that the particles segregate to the center of the PS domains (light regions). The staining of the PVP block interferes with the identification of gold particles in the PVP domains (dark regions), so the absence of PS-coated particles in the PVP domains was confirmed by TEM analysis of unstained samples (not shown). A histogram of particle center location as a function of distance from the center of the PS domain is shown in Figure 2b; the solid line is a Gaussian fit. As illustrated, the particle concentration is highest at the center of the PS domain (0 on the normalized x -axis) and falls to zero at the interfaces (± 1 on the x -axis) between the PS and PVP blocks. Analysis of PVP-coated particles in unstained PS-PVP diblock samples also reveals that those particles are located in the PVP domains as expected.

The localization of nanoparticles near the center of the polymer domain compatible with the particle surface coating is consistent with recent simulations.^{1,3} Particles coated with a given short homopolymer lower their enthalpy by segregating into the corresponding domain of the block copolymer. Furthermore, by concentrating particles near the *center* of the compatible domain where the polymer ends are located, the chains can accommodate particles by moving apart rather than by stretching. Localizing particles near the center of the compatible domain thus sacrifices translational entropy of the particles but avoids an even larger chain stretching penalty incurred by distributing particles throughout the domain.¹

In contrast to particles that are coated with either PS or PVP, particles that are coated with a *mixture* of PS and PVP thiols are localized at the interfaces between the PS-PVP blocks, as can be seen in Figure 2c. Analysis of the particle center locations in Figure 2d shows a sharp peak at the interface of the PS and PVP blocks, indicating strong adsorption of particles. This interfacial adsorption, which is not observed for pure PS or PVP thiol-coated particles,

[†] Department of Chemical Engineering.[‡] Department of Materials.

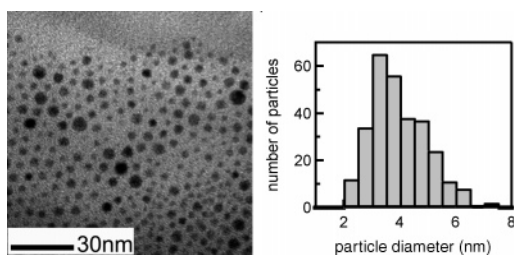


Figure 1. TEM image of PS ($M_n \sim 1300$ g/mol)-coated gold nanoparticles and the corresponding histogram of particle size distribution.

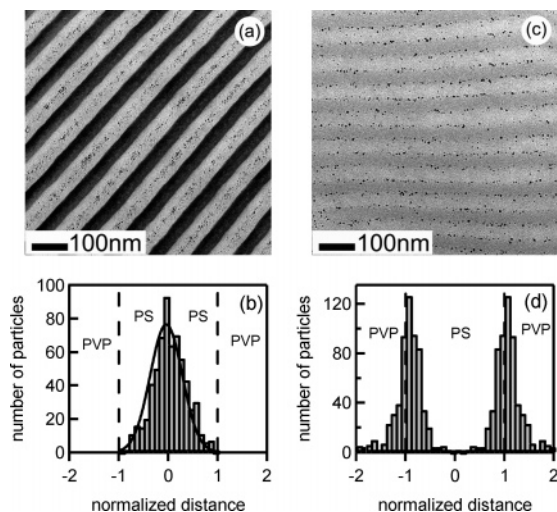


Figure 2. Cross-sectional TEM images of gold/block copolymer (PS-PVP diblock with $M_n \sim 196\,500$ g/mol) composite films using gold particles coated with (a) 100% PS thiol with a grafting density of ~ 0.14 chain/ \AA^2 , and (c) a 1:1 mixture of thiols that produces a particle coating that is 20% PVP with a grafting density of ~ 0.11 chain/ \AA^2 . Graphs (b) and (d) show the corresponding histograms of particle locations for samples (a) and (c), respectively.

can be understood in terms of γ_{SV} , γ_{NS} , and γ_{NV} , the interfacial energies of the PS-PVP diblock, the nanoparticle-PS, and the nanoparticle-PVP interfaces, respectively. The adsorption energy of a nanoparticle at an interface is given by $E_a = \pi r^2 \gamma_{SV} (1 - |\cos \theta|)^2$, where r is the radius of the particle, and $|\cos \theta| = |\gamma_{NV} - \gamma_{NS}| / \gamma_{SV}$.¹⁴ For particles coated with both PS and PVP, $\Delta\gamma \ll \gamma_{SV}$, so that $\cos \theta \ll 1$ and $E_a \approx \pi r^2 \gamma_{SV}$. Here, $2r \approx 8$ nm and $\gamma_{SV} \approx 2.8$ mN/m, which gives $E_a \sim 10k_B T$. Therefore, we expect the particles to be bound to the PS-PVP interface if $|\cos \theta|$ is small enough. Clearly, other factors can influence particle adsorption at the interface and may be necessary to explain why a nanoparticle with 80% surface coverage by PS still goes to the interface (Figure 2c). For example, any tendency of the PS and PVP thiols to segregate in 2D on the nanoparticle surfaces^{15–17} would further favor particle adsorption. By contrast, the chain

stretching free energy can be reduced if particles move away from the interface, as noted above. Further studies will be required to determine the importance of these and other factors on particle location.

In summary, we have designed a system consisting of a symmetric PS-PVP diblock copolymer matrix containing nanoparticles whose surfaces can be modified to be energetically similar to one of the blocks or amphiphilic with respect to the two blocks. Incorporating the particles into the block copolymer matrix, we demonstrated precise control of the location of the particles within the matrix simply by varying the composition of ligands on the particle surfaces. Particles with a mixture of PS and PVP thiols attached to the surfaces adsorb at the interfaces between the PS and PVP blocks. Particles with only PS or PVP thiol attached to the surfaces segregate near the center of the compatible domain. The control of particle location by varying compositions of ligands on the particle surfaces is a simple and versatile method that can be extended to other block copolymer and particle systems.

Acknowledgment. This work was supported in part by the U.S. Department of Energy under Award DE-F602-02ER45998, and the MRSEC Program of the National Science Foundation under Award DMR00-80034. This work made use of Central Facilities of the UCSB Materials Research Laboratory supported by the US NSF under Award DMR00-80034.

References

- (1) Thompson, R. B.; Ginzburg, V. V.; Matsen, M. W.; Balazs, A. C. *Science* **2001**, *292*, 2469–2472.
- (2) Lee, J. Y.; Thompson, R. B.; Jasnow, D.; Balazs, A. C. *Macromolecules* **2002**, *35*, 4855–4858.
- (3) Thompson, R. B.; Ginzburg, V. V.; Matsen, M. W.; Balazs, A. C. *Macromolecules* **2002**, *35*, 1060–1071.
- (4) Lauter-Pasyuk, V.; Lauter, H. J.; Ausserre, D.; Gallot, Y.; Cabuil, V.; Kornilov, E. I.; Hamdoun, B. *Phys. B* **1997**, *241*, 1092–1094.
- (5) Bronstein, L. H.; Sidorov, S. N.; Valetsky, P. M.; Hartmann, J.; Colfen, H.; Antonietti, M. *Langmuir* **1999**, *15*, 6256–6262.
- (6) Tsutsumi, K.; Funaki, Y.; Hirokawa, Y.; Hashimoto, T. *Langmuir* **1999**, *15*, 5200–5203.
- (7) Horiuchi, S.; Sarwar, M. I.; Nakao, Y. *Adv. Mater.* **2000**, *12*, 1507–1511.
- (8) Lopes, W. A.; Jaeger, H. M. *Nature* **2001**, *414*, 735–738.
- (9) Bockstaller, M. R.; Lapetnikov, Y.; Margel, S.; Thomas, E. L. *J. Am. Chem. Soc.* **2003**, *125*, 5276–5277.
- (10) Zhang, C. L.; Xu, T.; Butterfield, D.; Misner, M. J.; Ryu, D. Y.; Emrick, T.; Russell, T. P. *Nano Lett.* **2005**, *5*, 357–361.
- (11) Yee, C. K.; Jordan, R.; Ulman, A.; White, H.; King, A.; Rafailovich, M.; Sokolov, J. *Langmuir* **1999**, *15*, 3486–3491.
- (12) Brust, M.; Walker, M.; Bethell, D.; Schiffrin, D. J.; Whyman, R. *J. Chem. Soc., Chem. Commun.* **1994**, 801–802.
- (13) Stouffer, J. M.; McCarthy, T. J. *Macromolecules* **1988**, *21*, 1204–1208.
- (14) Pieranski, P. *Phys. Rev. Lett.* **1980**, *45*, 569–572.
- (15) Folkers, J. P.; Laibinis, P. E.; Whitesides, G. M. *Langmuir* **1992**, *8*, 1330–1341.
- (16) Stranick, S. J.; Parikh, A. N.; Tao, Y. T.; Allara, D. L.; Weiss, P. S. J. *Phys. Chem.* **1994**, *98*, 7636–7646.
- (17) Tamada, K.; Hara, M.; Sasabe, H.; Knoll, W. *Langmuir* **1997**, *13*, 1558–1566.

JA050376I